Computers and Chemical Engineering 23 (1999) 1031–1040

Computers & Chemical Engineering

www.elsevier.com/locate/compchemeng

Dynamic simulation of large boilers with natural recirculation

E.J. Adam, J.L. Marchetti *

Institute of Technologic Development for the Chemical Industry (INTEC), CONICET-Universidad Nacional del Litoral (U.N.L.), Güemes 3450, (3000) Santa Fe, Argentina

Received 17 October 1997; accepted 30 March 1999

Abstract

This paper presents a dynamic simulator of water-in-tube boilers with natural recirculation, the kind of equipment widely used in industries for steam generation either as a source of power or for providing heating capabilities in process plants. The development is based on a combination of two non-linear models, one for the evaporation in the vertical tubes and the other for the phase separation in the steam drum. An application is made to the boiler of a 30 MW thermoelectric power plant and the results are discussed. The dynamic responses of all variables show the consistency of the model representation with the expected behavior, including the effects of a PI level control adjusted using classic Ziegler–Nichols tuning rules.

Keywords: Boilers; Natural recirculation; Modeling and simulation

1. Introduction

The use of large boilers for steam generation is quite common in industry; they have received considerable attention from industry and academia since they frequently account for an important part of the overall fuel consumed in a plant. There are many applications in the chemical industry where utility steam is used for providing heat to the processes. Besides, the availability of steam at proper thermal conditions and rates is one of the critical features in the operation of every thermoelectric power plant. A dynamic simulator that is based on physical principles and keeps most non-linearities existing in the actual system serves as a useful benchmark allowing the analysis of the main dynamic characteristics of the operation. It also provides a medium for testing different control alternatives, evaluating optimization proposals, or helping to consider different safety procedures.

Even though there is a wide variety of designs, most of them include bundles of vertical tubes receiving the heat produced by several fuel burners. Steam is generated inside the tubes and goes up in a two-phase flow to a steam drum for phase separation. Several papers have previously presented linear and non-linear models of different steam generators. For instance TyssØ (1981) uses the extended Kalman filter for parameter estimation of a non-linear model; de Mello (1991) derives an interesting simplified model of a boiler with vertical tubes and natural recirculation, and Doñate and Moiola (1994) provided a rather simple model of a supercritical boiler.

The amount of details incorporated in the model of a simulator depends on the future use. For example, steam generators attached to nuclear reactors might need highly complex simulators oriented not only to describe the steam generation process but also to study the thermohydraulic details for safety analysis (RELAP-4, TRAC and Delhaye, Giot & Riethmuller, 1981), or to predict different characteristics of the two-phases flow (MINCS, Watanabe, Harino, Akimoto, Tanabe & Kohsaka, 1992).

If the goal is to design a control system to have the best possible performance, a realistic non-linear model is the appropriate support for simulations and testing. Very frequently, simple linear models obtained through some identification method and used for designing controllers are then used for testing procedures too. However, control design and tuning need realistic

* Corresponding author. Tel.: +54-342-4559174/77; fax: +54-342-4550944.

0098-1354/99/$ - see front matter
PII: S0098-1354(99)00269-0

simulations for a proper evaluation. A dynamic model for the simulation of steam generators with natural recirculation is presented here, that serves for the study and evaluation of control strategies. This is a halfway-complexity model developed to provide an adequate description of the operation and to give information about many important physical aspects.

This simulator is based on two models, one to describe the operation in the vertical tubes using mass, momentum and energy balances plus algebraic relationships to describe the phase change, and the other to represent the phase separation that takes place in the drum. Modeling the two-phase system has been the subject of studies by many investigators, and consequently several possibilities are available. The basic homogeneous mixture model (Delhaye et al., 1981) is used here for describing the vapor–liquid flow in the tubes, since it suffices for the requirements for the dynamic analysis of the operation. Concerning the phase separation, a non-linear model of the phenomena occurring in the steam drum has been developed. Then, both models are combined through additional statements rising from the overall mass and heat balances.

Finally, the boiler of a 30 MW power plant is simulated; since the liquid level in the steam drum has open-loop unstable characteristics, the results are obtained using a PI controller which actuates on the feed-water flow rate, i.e. the typical configuration implemented for level control in boilers.

2. Modeling the evaporation in vertical tubes

Fig. 1.a shows a sketch of the vertical tubes where most of the evaporation takes place. The model presented here is derived from more general time-space averaged field equations (Banerjee & Chan, 1980; Soria & De Lasa, 1991; Grau & Cantero, 1994), and is consistent with hypothesis adopted for the homogeneous-mixture model (Delhaye et al., 1981). The steady-state assumption was adopted after several evaluations of the associated time constants and comparing with the dynamics in the separation drum.

2.1. Balance equations

Differential mass, energy and momentum balance equations for steady-state conditions are used for modeling the two-phase flow in the vertical tubes. According to the homogeneous-mixture model, the changes in the two-phase flow properties occur along the tubes only, i.e. as the z-coordinate varies.

Hence, the mass balance equation for the mixture is,

$$\frac{\mathrm{d}}{\mathrm{d}z}[\varepsilon_g\rho_g u + (1-\varepsilon_g)\rho_l u] = 0, \tag{1}$$

where u is the velocity of the homogeneous mixture and ε_g is the vapor–void fraction.

The momentum balance equation for the mixture is,

$$\frac{\mathrm{d}}{\mathrm{d}z}[\varepsilon_g\rho_g u^2 + (1-\varepsilon_g)\rho_l u^2] + \frac{\mathrm{d}}{\mathrm{d}z}[P] = -[\varepsilon_g\rho_g + (1-\varepsilon_g)\rho_l]g - \tau_{\mathrm{wm}}, \tag{2}$$

where P is the local pressure and τ_{wm} is the wall-shear stress per unit of volume, and the energy balance equation for the mixture is written as follows:

$$\frac{\mathrm{d}}{\mathrm{d}z}\left[\varepsilon_g\rho_g u\left(\hat{H}_g + \frac{1}{2}u^2\right)\right] + \frac{\mathrm{d}}{\mathrm{d}z}\left[(1-\varepsilon_g)\rho_l u\left(\hat{H}_l + \frac{1}{2}u^2\right)\right] = \dot{q}_{\mathrm{wm}} - [\varepsilon_g\rho_g + (1-\varepsilon_g)\rho_l]ug \tag{3}$$

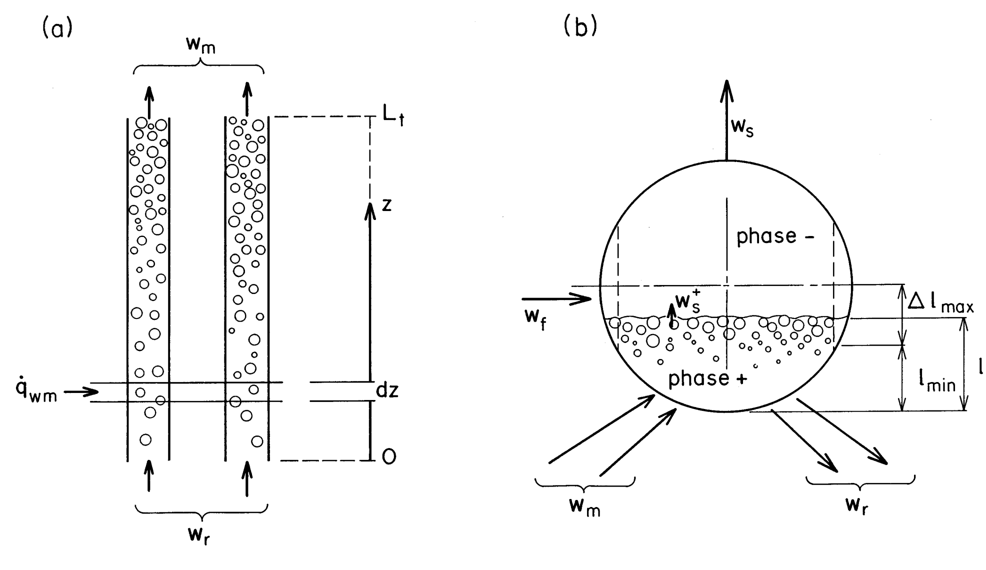

Fig. 1. (a) Vertical tubes scheme. (b) Steam drum scheme.

where $\hat{H}$ stands for enthalpy per unit mass and $\dot{q}_{wm}$ is the heat flux at the tube wall per unit of volume.

2.2. Algebraic equations

The model requires additional relationships for the complete description, most of them showing non-linear forms. For instance, the equilibrium curve is represented by the Wagle's correlation (Wagle, 1985),

$$T = T_b[1 + a_1 \ln(P_{rel}) + a_2 \ln^2(P_{rel}) + a_3 \ln^3(P_{rel}) + a_4 \ln^4(P_{rel})] \quad (4)$$

where P_{rel} is a relative pressure and T_b is the equilibrium temperature at the reference pressure.

The state equation for the vapor phase is written as,

$$PM = Z\rho_g RT, \quad (5)$$

where Z is the compressibility factor defined according to classical texts (Reid, Prausnitz & Poling, 1987) and taken as a constant value in this work.

Also, two constitutive equations are necessary, one is for the friction factor that helps to describe the pressure drop along the tubes, and the other for determining the heat-transfer film coefficient to estimate the heat flow from the wall. The appropriate evaluation of these parameters is very important to achieve a good model representation.

The evaluation of τ_{wm} is made through the calculation of the pressure loss by friction,

$$\tau_{wm} = \left(\frac{2f}{d_t}\right)(\rho_m u^2) \quad (6)$$

using the friction factor correlated by Dukler, Wicks and Cleveland (1964) for the homogeneous mixture model,

$$f = 0.0014 + 0.125\mathrm{Re}^{-0.32} \quad (7)$$

The density and viscosity of the mixture used to compute Eq. (6) and the Reynolds number in Eq. (7) are calculated as follows:

$$\mu_m = \varepsilon_g \mu_g + (1 - \varepsilon_g)\mu_l \quad (8)$$

$$\rho_m = \varepsilon_g \rho_g + (1 - \varepsilon_g)\rho_l \quad (9)$$

Besides, it is necessary to estimate the heat flux from the tube wall, a quantity that is a function of several variables like the vapor–void fraction, the velocity of the mixture, the local temperature and phase properties, etc. A classical constitutive equation is used here,

$$\dot{q}_{wm} = \left(\frac{\pi\ d_t}{A_t}\right)U_{wm}[T_w - T] \quad (10)$$

where the global heat transfer coefficient is evaluated through the relationship,

$$\frac{1}{U_{mw}} = \frac{1}{h_m} + W \quad (11)$$

Since we focus on changes occurring inside the tube, Eq. (11) emphasizes the dependence on the internal film coefficient leaving all other resistance component in the constant term W. The internal local film coefficient is then evaluated through the equation of Dittus and Boelter (1930) using a modified Reynolds number (Wadeker, 1993),

$$h_m = 0.023\frac{k_l}{d_t}\mathrm{Re}_m^{0.8}\mathrm{Pr}_l^{0.4}, \quad (12)$$

$$\mathrm{Re}_m = \frac{d_t G_m \rho_l}{\mu_l}\left(\frac{x}{\rho_g} + \frac{1 - x}{\rho_l}\right), \quad (13)$$

where x is the vapor quality.

Numerical simulation of the evaporation in vertical tubes using this set of modeling equations show good agreement with results of experimental data, as shown by Adam and Marchetti (1995). Concerning the balance of equations and unknowns for this model we refer to Adam and Marchetti (1994).

3. Modeling the phase separation in the drum

This section presents a dynamic model of the phase separation in the drum. Typically, the drum is an accumulating tank located at the top of a boiler that receives the vapor–liquid mixture coming from the tubes, separates one from the other, and attenuates steam demand disturbances. The following are assumptions made for modeling the operation in the tank: (i) the drum is adiabatic; (ii) pressure and temperature are uniform in both phases; (iii) the vapor in the drum is described by the perfect gas equation; (iv) pressure losses by friction or pressure changes due to hydrostatic variations are negligible.

3.1. Balance equations

Fig. 1b shows an schematic of the drum where the phase separation takes place. It has two inlet streams: the mixed phase flow coming from the vertical tubes w_m and the feed-water w_f. There are also two outlet streams: the recirculating flow w_r and the produced steam w_s leaving the drum. The figure also shows two important design specifications; Δl_{max}, which indicates the maximum change expected for the level of the liquid–vapor mixture, and l_{min} which is the minimum expected value for this level.

Hence, the balance equations are written following the above hypothesis and according to the scheme and nomenclature shown in Fig. 1b:

Total mass balance,

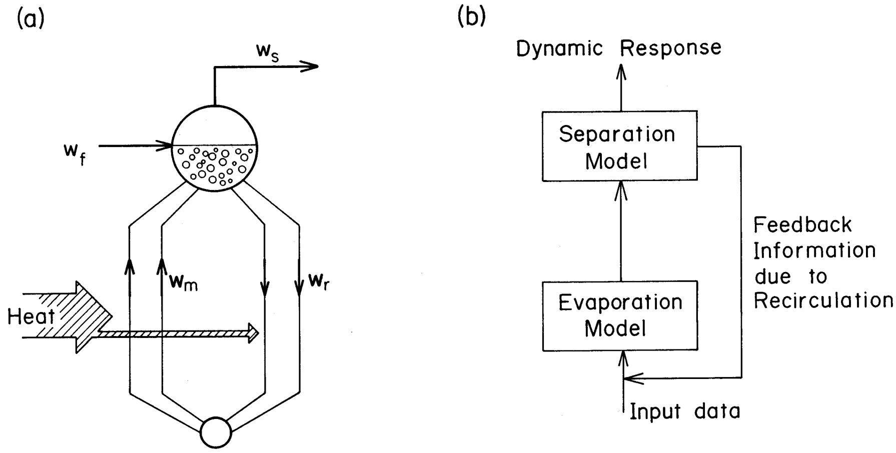

Fig. 2. (a) Boiler scheme. (b) Structure of the non-linear simulator.

$$\frac{d(M_{\mathrm{tot}})}{dt} = w_{\mathrm{f}} + w_{\mathrm{m}} - w_{\mathrm{s}} - w_{\mathrm{r}}. \tag{14}$$

Mass balance for the liquid–vapor mixture,

$$\frac{d(M_{\mathrm{tot}}^{+})}{dt} = w_{\mathrm{f}} + w_{\mathrm{m}} - w_{\mathrm{s}}^{+} - w_{\mathrm{r}}. \tag{15}$$

Total energy balance,

$$\frac{d(H_{\mathrm{tot}})}{dt} = w_{\mathrm{f}}\hat{H}_{\mathrm{f}} + w_{\mathrm{m}}\hat{H}_{\mathrm{m}} - w_{\mathrm{s}}\hat{H}_{\mathrm{s}} - w_{\mathrm{r}}\hat{H}_{\mathrm{r}}. \tag{16}$$

3.2. Algebraic equations

Equations defining M_{tot}, M_{tot}^{+}, and H_{tot} are,

$$M_{\mathrm{tot}} = V_{\mathrm{l}}^{+}\rho_{\mathrm{l}} + V_{\mathrm{g}}^{+}\rho_{\mathrm{g}} + V_{\mathrm{g}}^{-}\rho_{\mathrm{g}}, \tag{17}$$

$$M_{\mathrm{tot}}^{+} = V_{\mathrm{l}}^{+}\rho_{\mathrm{l}} + V_{\mathrm{g}}^{+}\rho_{\mathrm{g}}, \tag{18}$$

$$H_{\mathrm{tot}} = V_{\mathrm{l}}^{+}\rho_{\mathrm{l}}\hat{H}_{\mathrm{l}} + V_{\mathrm{g}}^{+}\rho_{\mathrm{g}}\hat{H}_{\mathrm{g}} + V_{\mathrm{g}}^{-}\rho_{\mathrm{g}}\hat{H}_{\mathrm{g}}. \tag{19}$$

Notice that the hypothesis of uniform pressure allows the assumption that steam density is independent of the height, even though there are bubbles all over in the volume of mixture. An additional relationship linking the above equations sets the constant condition for the total volume of the drum,

$$V_{\mathrm{sep}} = V_{\mathrm{l}}^{+} + V_{\mathrm{g}}^{+} + V_{\mathrm{g}}^{-}. \tag{20}$$

3.3. Constitutive equations

Due to the model structure, a constitutive equation is necessary for determining the steam mass flow rate, w_s^{+}, between the liquid–vapor mixture (+ phase) and the vapor phase (− phase), as well as for determining the recirculating liquid flow rate.

The steam-mass flow rate leaving the mixture can be assumed as being proportional to the average surface fraction $\tilde{A}_{\mathrm{sep}}$ occupied by the bubbles, i.e.

$$w_{\mathrm{s}}^{+} = \tilde{A}_{\mathrm{sep}}\left(\frac{V_{\mathrm{g}}^{+}}{V_{\mathrm{l}}^{+} + V_{\mathrm{g}}^{+}}\right)u_{\mathrm{g}}^{+}\rho_{\mathrm{g}}, \tag{21}$$

where, for steam–water flows at high-pressure, the drag velocity u_{g}^{+} can be estimated as follows (Zuber & Findlay, 1965):

$$u_{\mathrm{g}}^{+} = 1.41\left(\frac{\sigma g(\rho_{\mathrm{l}} - \rho_{\mathrm{g}})}{\rho_{\mathrm{l}}^{2}}\right)^{1/4}. \tag{22}$$

Besides, the cylindrical drum geometry (see Fig. 1b) leads to defining the mean total area by,

$$\tilde{A}_{\mathrm{sep}} = L_{\mathrm{sep}}\sqrt{d_{\mathrm{sep}}^{2} - \Delta l_{\mathrm{max}}^{2}}. \tag{23}$$

The natural recirculation in boilers is due to the difference between the liquid density of the returning flow (see Fig. 2a) and the average density of the mixture in the vertical tubes. The flow rate, in this case, is proportional to the square root of such difference (TyssØ, 1981),

$$w_{\mathrm{r}} = K\sqrt{\rho_{\mathrm{l}} - \rho_{\mathrm{ave}}}. \tag{24}$$

The average density in the vertical tubes is computed by,

$$\rho_{\mathrm{ave}} = \frac{\rho_{\mathrm{m}} + \rho_{\mathrm{l}}}{2}, \tag{25}$$

where ρ_m is evaluated using Eq. (9) at the tube outlets, and the constant K is based on satisfying steady-state conditions.

The two-phase stream coming from the vertical tubes is completely determined by the evaporation model. Therefore, the mass flow rate is computed by,

$$w_{\mathrm{m}} = N_{\mathrm{t}}A_{\mathrm{t}}\rho_{\mathrm{m}}u, \qquad \text{at } z = L_{\mathrm{t}}, \tag{26}$$

which obviously depends on the tube-outlet conditions, i.e. it might change with time.

Other variables are treated as follows: (i) the feed-water flow rate is a known stream that later becomes the manipulated variable for level control; (ii) the produced steam flow rate is taken as a load variable since it is the main disturbance when changing the steam demand; (iii) vapor and liquid enthalpies are calculated as functions of temperature in the classical form; and (iv) the liquid–vapor equilibrium curve is computed as following Wagle (1985).

From the control point of view, the variable of interest is the level of the liquid–vapor mixture (+ phase). The stability and performance of the level control system is of primary importance for the operation of boilers. In order to allow the dynamic analysis of this problem, we introduced the following definition of the level of the liquid–vapor mixture in the drum (see Fig. 1b):

$$l = l_{\min} + \frac{V_l^+ + V_g^+ - V_{\min}}{\tilde{A}_{\text{sep}}}, \tag{27}$$

where $V_{\min}$ is the volume corresponding to the reference $l_{\min}$.

This separation drum model has nine unknowns; M_{tot}, M_{tot}^+, H_{tot}, w_s^+, w_r, V_l^+, V_g^+, V_g^-, and l, while Eqs. (14)–(19), Eq. (21), Eq. (24) and Eq. (27) give a system of three non-linear differential equations and six non-linear algebraic equations. Note that all properties or variables associated to inlet or feed flows are part of the available data at each time instant the model is solved.

4. Non-linear model of a boiler

Fig. 2a shows a simplified scheme of a boiler where the main parts are: (i) the vertical tubes where the evaporation takes place; (ii) the separation drum where the vapor separates from the boiling liquid; and (iii) the connection for the natural recirculation. The models discussed above are solved sequentially at each time instant, as represented in Fig. 2b. As mentioned before, comparative small time constants allow the insertion of the steady-state evaporation model into the structure of the overall boiler model where the main dynamics are described by the separation drum model. Hence, under non-stationary conditions, the evaporation model gives different output values for each time instant. This reduces computing times significantly allowing an efficient model combination for describing the overall dynamics.

The natural recirculation was described under the hypothesis that saturated liquid at the bottom pressure defines the stream condition at the inlet of the vertical tubes. Since the recirculating liquid leaves the separator at the pressure in the top, the principal change in this stream is due to the pressure difference. This stream would be subcooled when reaching the bottoms if no other adjustment is made, but due to constructive characteristics of most of these type of boilers, it receives a small fraction of heat (as compared to the overall energy released by the burners) upon returning toward the tube entries. This consideration gives support to the assumption that the recycled liquid, when reaching the lower part of the boiler, is close to the saturated condition. Hence, the simulator steps continuously on the saturated condition at the evaporation tube inlets, but following pressure variations in the upper part of the boiler, and taking the necessary energy for reaching saturation out of the heat delivered for evaporation. Pressure drop along the recirculating path has been assumed negligible due to wider cross section areas in the circuit.

5. Numerical strategies

5.1. Numerical strategy for the evaporation model

Two numerical strategies were proposed for solving the combined system of differential and algebraic equations (Adam & Marchetti, 1994; Adam, Marchetti, Pérez & Martínez, 1994). In this case we decided to compute analytically all the derivatives in an explicit form, such that,

$$\frac{d\mathbf{y}(z)}{dz} = \mathbf{A}(z)^{-1}\mathbf{b}(z), \qquad \mathbf{y}_0 = \mathbf{y}(z=0), \tag{28}$$

where $\mathbf{A}$, $\mathbf{b}$ and the integrating variables are given in Appendix B Then, an automatic step-size 4th-5th-order Runge–Kutta integration method is used up to $z = L_t$. This results in a simple and robust method to obtain the vapor–liquid mixture condition at the tube outlets.

5.2. Numerical strategy for the separator model

The equation system defining the boiler-drum model is written following the state space representation,

$$\frac{d\mathbf{x}(t)}{dt} = \mathbf{f}(\mathbf{x}(t)) + \mathbf{g}_1 m(t) + \mathbf{g}_2\delta_1(t) + \mathbf{g}_3 m(t)\delta_2(t) \tag{29}$$

$$l(t) = l(\mathbf{x}(t)) \tag{30}$$

The state variables in this case are (see Appendix C): (i) the total mass in the drum; (ii) the total mass in the + phase, and (iii) the total enthalpy in the drum. The disturbances to the system are the steam flow-rate ($\delta_1(t)$), and the feed-water temperature ($\delta_2(t)$). The feed-water flow-rate is the manipulated variable, $m(t)$, for level control purposes.

Stepping on data at the time instant k, an automatic step-size 4th–5th order Runge–Kutta integration method is used on Eq. (29) to find the unknowns at $k+1$. Then the Newton–Rapson method is applied to a set of algebraic non-linear equations represented through Eq. (30). The numerical methods were taken from Ralston and Rabinowitz (1978) and Holland and Liapis (1983).

6. Simulation results

The characteristic dimensions and operating conditions of the boiler of a 30 MW thermoelectric power plant located in Santa Fe (Argentina) are used for testing and verification of the above combined non-linear model. Like most boilers, the level of liquid in the drum is open loop unstable, and consequently a PI controller is used for stabilization by manipulating the feed-water flow-rate through a small time delay ($T_d =$ 5 s)) representing the control valve ($K_v = 1$) (see Fig. 3). The controller tuning is accomplished through the method of Ziegler and Nichols (1942) i.e. numerical experiences were run in the simulator to determine the ultimate gain and period. Typically, the flow rate of fuel delivered for combustion is another important manipulated variable, particularly for controlling the outlet steam pressure. In this work however, we take the heat flow rate as a load variable and the pressure is in open loop.

6.1. Load disturbance 1

The dynamic behavior of the main variables in the boiler when receiving a change of + 5% in the steam demand is first simulated. Some physical dimensions and stream conditions for the problem are shown in Table 1. Fig. 4a shows the dynamic response of the level variable to a positive 5% step change in the steam flow-rate, this is the typical inverse response in steam generators for a sudden increase in the demand also known as the 'swell and shrink' phenomena. Fig. 4b shows how the drum pressure falls since there is not pressure control actuating on the heat input, i.e. the boiler provides more steam but loosing quality.

Fig. 5 shows the dynamic responses of the state variables in the separation model. Notice in Fig. 5a, that even though the new steady state keeps the required level, the amounts of total accumulated mass in the drum and the total accumulated mass of the + phase are lower than at their values at the initial point. In Fig. 5b, the accumulated enthalpy follows a similar evolution pattern.

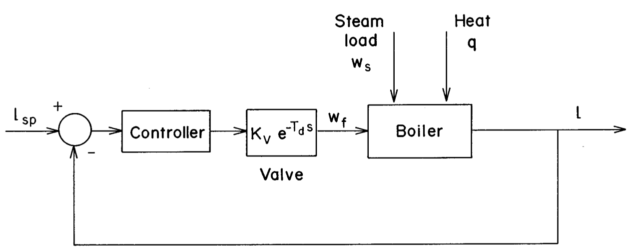

Fig. 3. Block diagram of the level control loop.

Table 1
Design parameters and operating conditions of the simulated boiler

Parameters	Value
Vertical tubes	
Length,	25.0 m
Diameter, d_t	0.0508 m
Number of tubes, N_t	440
Separation drum	
Length, L_{sep}	8.0 m
Diameter, d_{sep}	1.8 m
Height of mixed phase, l_{sep}	0.70 m (*)
Feed water stream	
Flow, w_f	27.778 (kg s^{-1})
Pressure, P_f	1.2156 10^7 (Pa)
Temperature, T_f	503.16 (K)
Vapor stream	
Pressure (drum pressure), P_s	8.4 10^6 (Pa)
Temperature (drum temp.), T_s	571.3 (K)
Delivered energy	
Heat flow to the tubes	2.61 10^4 W m^{-2}

* Nominal steady state.

Since there is a misleading initial increase of the level, Fig. 6 shows that the controller starts reducing the feed-water flow-rate, but as soon as the level changes the trend the water inlet to the system increases as expected. This figure also shows how the mass balance closes at the new steady state since both the steam and the feed-water flow-rates go to the same steady value.

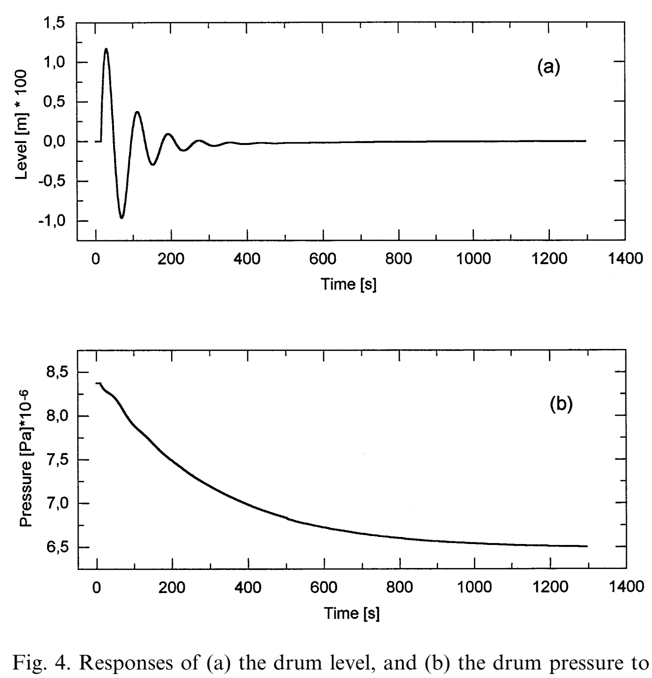

Fig. 4. Responses of (a) the drum level, and (b) the drum pressure to 5% step change in the steam load.

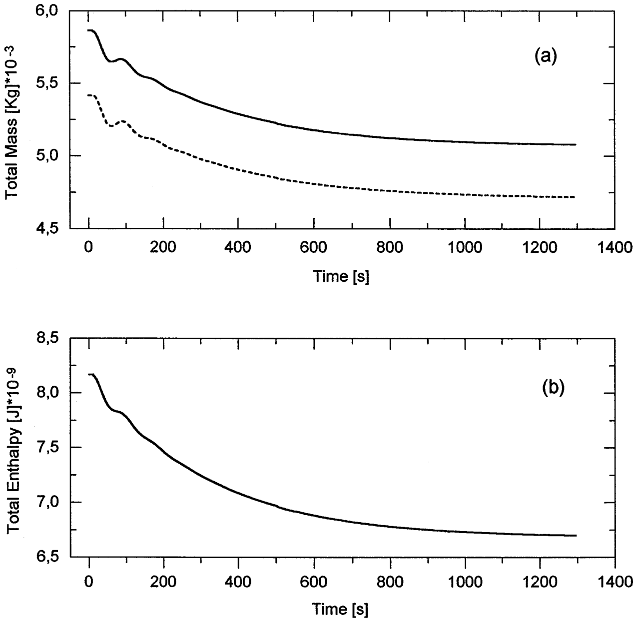

Fig. 5. (a) Responses of the accumulated total mass (—) and the total mass of the phase = (----). (b) Response of the total enthalpy accumulated to a 5% step change in the steam load.

6.2. Load disturbance 2

Given the same starting condition, a positive 5% increase in the heat input is introduced while keeping the same steam mass flow-rate. Fig. 7a shows the level moving initially up but then returning to the desired set point after several oscillations. Fig. 7b confirms that the steam pressure goes up since the pressure controller is in open loop for this run. Hence, the main final stationary effect is the production of a higher quality steam at the original flow-rate.

The dynamic responses of the drum-model state variables are shown in Fig. 8. Notice that there is an increment of the accumulated enthalpy, and a slow growth in the total accumulated mass in the drum. Also, inspection of Fig. 9 shows that the level controller initially reduces the feed-water flow-rate in order to avoid the level increase in the separator, but it returns to the initial value due to the fact that there is no change in the steam demand.

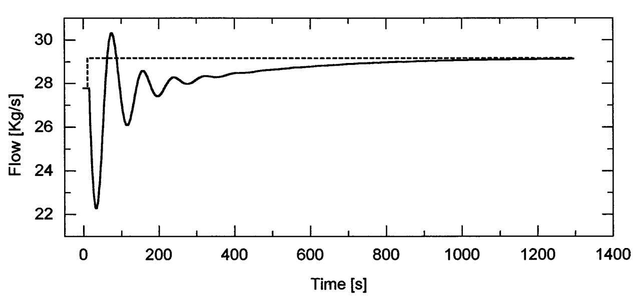

Fig. 6. Change in the steam load (----) and response of the feed-water flow rate (—).

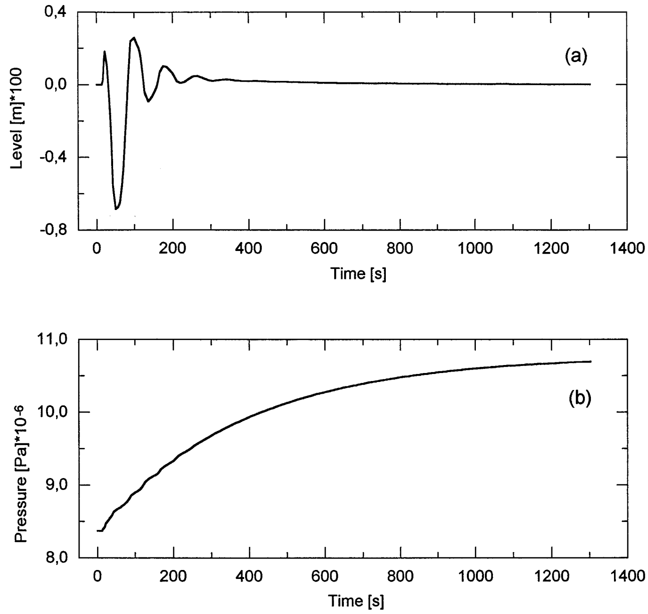

Fig. 7. Responses of (a) the drum level, and (b) the drum pressure to a 5% step change in the heat input.

Though the results of this second test are quite coherent with the expected behavior it should be observed that the model described above does not include, at the present time, an extra lag existing in the real operation between the fuel valves and the tube-wall temperature. This part of the modeling task is a matter of future work including specific control structures for attending safety considerations and combustion efficiency problems.

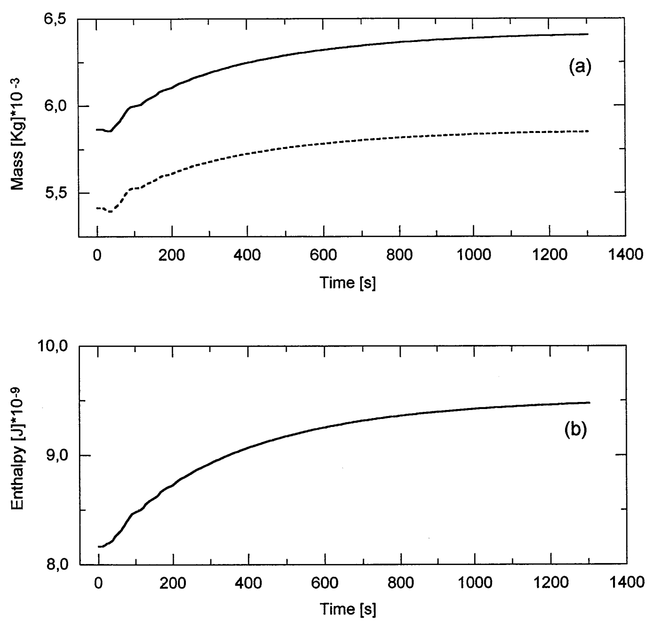

Fig. 8. (a) Responses of the accumulated total mass (—) and the total mass of the phase = (----). (b) Response of the total enthalpy accumulated to a 5% step change in the heat input.

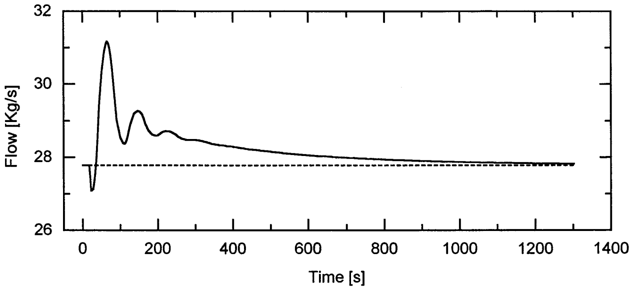

Fig. 9. Response of the feed-water flow rate (—), without changing the steam load (---).

7. Conclusions

Two non-linear models, one for the evaporation in tubes and the other for the steam separation in a drum, were combined to yield a dynamic model of large boilers. The development serves to simulate the water-side dynamic operation of steam generators whose design is based on: (i) vertical tubes exposed to a source of heat like fuel burners; (ii) a separation drum; and (iii) natural recirculation of the liquid hold-up. The main purpose of this work is to provide a useful tool for studying and analyzing different control strategies in order to achieve high control performance, particularly for level and pressure control under steam demand changes.

The dynamic behavior of every physical variable analyzed through the proposed model is satisfactory and consistent with the practical experience. Variables with doubtful behaviors such as the inverse response of the mixed-phase level in the drum, or steam quality variations are efficiently described.

The results of numerical simulations presented in this paper show the dynamics of most important variables in the boiler of a 30 MW thermoelectric power plant under two frequent load changes: (i) a positive increase in the steam demand; and (ii) a positive increment in the heat input to the vertical tubes. In both cases, a simple PI controller is used for stabilizing the mixed-phase level in the drum while the pressure control loop is open. For additional control analysis modeling of lags existing on the fire-side of the boiler furnace could be necessary depending on the pattern under which the energy is delivered up to the tubes.

Acknowledgements

The authors thank CONICET and Universidad Nacional del Litoral (UNL) for the economic support received. They want also to acknowledge EE Arnoldo Reutemann of Centrales Térmicas del Litoral for providing the operative and technical data for the application example.

Appendix A. Nomenclature

a_i	equilibrium curve coefficients in Eq. (4), $i=1$ to 4
A	section area (m^2)
$\mathbf{A}$	matrix of the evaporation model
$\boldsymbol{b}$	vector of independent terms in the evaporation model
c_p	heat capacity at constant pressure (J kg^{-1} K^{-1})
D	diameter (m)
f	Dukler friction factor
$\mathbf{f}$	function of several variables in Eq. (29)
g	standard gravity (m s^{-2})
$\mathbf{g}_i$	vectors in Eq. (29) and defined by (A-2), $i=1$ to 3.
G	mass flux (kg m^{-2}s^{-1})
h	heat transfer film coefficient (W m^{-2} K^{-1}).
$\hat{H}$	enthalpy per unit mass (J kg^{-1})
K	proportional constant in Eq. (24), (kg s^{-1})/(kg m^{-3})$^{1/2}$
k	conductivity (W m^{-1} K^{-1})
l	level of the vapor–liquid mixture in the separation drum (m)
L	length (m)
m	manipulated variable
M	accumulated mass (kg)
P	pressure (Pa)
$\dot{q}$	heat input per unit of volume (W m^{-3})
Re	Reynolds number
t	time (s)
T	temperature (K)
U	global heat transfer coefficient, W m^{-2} K^{-1}
u	velocity (m s^{-1})
V	volume (m^3)
w	mass flow rate (kg s^{-1})
W	tube wall heat transfer resistance (m^2 K W^{-1})
x	vapor quality
$\mathbf{x}$	state vector in Eq. (29)
$\mathbf{y}$	vector of integrating variables in Eq. (28)
z	axial or vertical coordinate in the evaporation model (m)

Greeks

δ	disturbance
ε	volume fraction of vapor in the tubes
λ	latent heat of vaporization (J kg^{-1})
ρ	density (kg m^{-3})
σ	surface tension (N m^{-1})
τ	wall shear stress per unit of volume (Pa m^{-3})

Subscripts

b	a given reference point in the liquid–vapor equilibrium curve
f	feed
g	vapor or gas phase
l	liquid phase
m	mixed phase
r	recirculation
s	steam
sep	separator or drum
t	tubes
tot	total
v	vapor phase
w	wall
0	initial condition

Superscript

+	liquid–vapor mixture in the drum
−	vapor phase in the drum

Appendix B. The evaporation model

The relationships presented in this appendix describe Eqs. (28)–(30) for easy implementation of the proposed models in simulation experiences.The components of vector **y**, in the Eq. (28) are:

$\mathbf{y}_1 = \varepsilon_g,$

$\mathbf{y}_2 = \rho_g,$

$\mathbf{y}_3 = u,$

$\mathbf{y}_4 = T,$

$\mathbf{y}_5 = P.$

The following are the coefficients of the **A** matrix in Eq. (28):
from Eq. (1),

$A_{11} = (\rho_g - \rho_l)u,$

$A_{12} = \varepsilon_g u,$

$A_{13} = \varepsilon_g\rho_g + (1-\varepsilon_g)\rho_l,$

$A_{14} = 0,$

$A_{15} = 0.$

From Eq. (3) we obtain,

$$A_{21} = \left\{\rho_g\left[c_p^l(T-T_0) + \lambda_v + \frac{1}{2}u^2\right]\right\}u - \left\{\rho_l\left[c_p^l(T-T_0) + \frac{1}{2}u^2\right]\right\}u,$$

$$A_{22} = \varepsilon_g u\left[c_p^l(T-T_0) + \lambda_v + \frac{1}{2}u^2\right],$$

$$A_{23} = \varepsilon_g\rho_g\left[c_p^l(T-T_0) + \lambda_v + \frac{3}{2}u^2\right] + (1-\varepsilon_g)\rho_l\left[c_p^l(T-T_0) + \frac{3}{2}u^2\right],$$

$A_{24} = [\varepsilon_g\rho_g c_p^g + (1-\varepsilon_g)\rho_l c_p^l]u,$

$A_{25} = 0.$

From Eq. (2),

$A_{31} = (\rho_g - \rho_l)u^2,$

$A_{32} = \varepsilon_g u^2,$

$A_{33} = 2[\varepsilon_g\rho_g + (1-\varepsilon_g)\rho_l]u,$

$A_{34} = 0,$

$A_{35} = 1.$

From Eq. (4),

$A_{41} = 0,$

$A_{42} = 0,$

$A_{43} = 0,$

$A_{44} = 1,$

$$A_{45} = -\frac{T_b}{P}[a_1 + 2a_2\ln(P/P_b) + 3a_3\ln^2(P/P_b) + 4a_4\ln^3(P/P_b)].$$

And from Eq. (5),

$A_{51} = 0,$

$A_{52} = 1,$

$A_{53} = 0,$

$A_{54} = \rho_g/T,$

$A_{55} = -\rho_g/P.$

The following are the elements of the vector ***b*** in Eq. (28):

$b_1 = 0,$

$$b_2 = \left(\frac{4}{d_t}\right)U_{wm}[T_w - T] - [\varepsilon_g\rho_g + (1-\varepsilon_g)\rho_l]ug,$$

$$b_3 = -[\varepsilon_g\rho_g + (1-\varepsilon_g)\rho_l]g - \left(\frac{4f}{d_t}\right)\left\{\frac{1}{2}[\varepsilon_g\rho_g + (1-\varepsilon_g)\rho_l]u^2\right\},$$

$b_4 = 0,$
$b_5 = 0.$

Appendix C. The separation model

Eqs. (14)–(16) define state variables that can be written as,

$$\frac{d}{dt}\begin{pmatrix} M_{tot} \\ M_{tot}^+ \\ H_{tot} \end{pmatrix} = \begin{pmatrix} w_m - w_r \\ w_m - w_s^+(M_{tot}, M_{tot}^+) - w_r \\ w_m\hat{H}_m - w_r\hat{H}_r \end{pmatrix}$$

$$+\begin{pmatrix} w_{\mathrm{f}} \\ w_{\mathrm{f}} \\ 0 \end{pmatrix} + \begin{pmatrix} -w_{\mathrm{s}} \\ 0 \\ -w_{\mathrm{s}}\hat{H}_{\mathrm{s}} \end{pmatrix} + \begin{pmatrix} 0 \\ 0 \\ w_{\mathrm{f}}\hat{H}_{\mathrm{f}} \end{pmatrix}, \qquad \text{(A-1)}$$

or,

$$\frac{\mathrm{d}}{\mathrm{d}t}\begin{pmatrix} M_{\mathrm{tot}} \\ M^{+}_{\mathrm{tot}} \\ H_{\mathrm{tot}} \end{pmatrix} = \begin{pmatrix} w_{\mathrm{m}} - w_{\mathrm{r}} \\ w_{\mathrm{m}} - w^{+}_{\mathrm{s}}(M_{\mathrm{tot}}, M^{+}_{\mathrm{tot}}) - w_{\mathrm{r}} \\ w_{\mathrm{m}}\hat{H}_{\mathrm{m}} - w_{\mathrm{r}}\hat{H}_{\mathrm{r}} \end{pmatrix}$$

$$+\begin{pmatrix} 1 \\ 1 \\ 0 \end{pmatrix} w_{\mathrm{f}} + \begin{pmatrix} -1 \\ 0 \\ -\hat{H}_{\mathrm{s}} \end{pmatrix} w_{\mathrm{s}} + \begin{pmatrix} 0 \\ 0 \\ 1 \end{pmatrix} w_{\mathrm{f}}\hat{H}_{\mathrm{f}}, \qquad \text{(A-2)}$$

which is Eq. (29). Furthermore, Eq. (30) represents to Eq. (27) where V^{+}_{l} and V^{+}_{g} are function of the above states variables $\mathbf{x} = [M_{\mathrm{tot}}, M^{+}_{\mathrm{tot}}, H_{\mathrm{tot}}]$,

$$l(\mathbf{x}) = l_{\min} + \frac{V^{+}_{l}(\mathbf{x}) + V^{+}_{g}(\mathbf{x}) - V_{\min}}{\tilde{A}_{\mathrm{sep}}}$$

Once $\mathbf{x}$ is determined for time $t+1$, V^{+}_{l} and V^{+}_{g} are obtained by solving Eqs. (17)–(20) together with Eqs. (4) and (5) and using an appropriate solver for simultaneous nonlinear equation sets.

References

Adam, E. J., & Marchetti, J. L. (1994). Modelo estacionario de evaporación en tubos verticales. *CIT-Información Tecnológica*, *5*, 67–76.

Adam, E. J., Marchetti, J. L., Pérez, G., & Martínez, E. (1994). Estudio de los problemas numéricos en un modelo de evaporación en tubos verticales, MECOM-IV Congreso de Mecánica Computacional. *Mecánica Computacional*, *14*, 404–413.

Adam, E. J., & Marchetti, J. L. (1995). Simulation of the incipient boiling phenomenon in vertical tubes. *Latin American Applied Research*, *25*, 237–242.

Banerjee, S., & Chan, M. C. (1980). Separated flow models-I: analysis of the averaged and local instantaneous formulations. *International Journal of Multiphase Flow*, *6*, 1–24.

Dukler, A. E., Wicks, M., & Cleveland, R. G. (1964). Friccional pressure drop in two-phase flow: B. an approach through similarity analysis. *American Institute of Chemical Engineers Journal*, *10*, 44–51.

Delhaye, J. M., Giot, M., & Riethmuller, M. L. (1981). *Thermohydraulics of two-phase systems for industrial design and nuclear engineering*. New York: McGraw-Hill.

de Mello, F. P. (1991). Boiler models for system dynamic perfomance studies. *IEEE Transactions on Power Apparatus and Systems*, *6*, 66–74.

Dittus, F., & Boelter, L. M. K. (1930). *Heat transfer in automobile radiators of tubular type* (p. 443). Berkeley: Publications Engineering, University of California.

Doñate, P. D., & Moiola, J. L. (1994). Model of a once-through boiler for dynamic studies. *Latin American Applied Research*, *24*, 159–166.

Grau, R. J., & Cantero, H. J. (1994). A systematic time-, space- and time-space-averaging procedure for bulk phase equations in systems with multiphase flow. *Chemical Engineering Science*, *49*, 449–461.

Holland, C. D., & Liapis, A. I. (1983). *Computer methods for solving dynamic separation problems*. New York: McGraw-Hill.

Ralston, A., & Rabinowitz, P. (1978). *A first course in numerical analysis*. New York: McGraw-Hill.

Reid, R. C., Prausnitz, J. M., & Poling, B. E. (1987). *The properties of gases and liquids* (4th ed.). New York: McGraw-Hill.

Soria, A., & De Lasa, H. I. (1991). Averaged transport equations for multiphase systems with interfacial effects. *Chemical Engineering Science*, *46*, 2093–2111.

TyssØ, A. (1981). Modelling and parameter estimation of a ship boiler. *Automatica*, *17*, 157–166.

Wadeker V. (1993) Onset of boiling in vertical up-flow, In *American Institute of Chemical Engineers Symposium Series*, *Heat Transfer*, (pp. 293–299). Atlanta.

Wagle, M. P. (1985). Predict saturation temperature as a function of vapor pressure. *Chemical Engineering*, *92*, 77–80.

Watanabe, T., Harino, M., Akimoto, M., Tanabe, F., & Kohsaka, A. (1992). Two-phase flow characteristics analysis code. *JAERI*, *1326*, 1–232.

Ziegler, J. G., & Nichols, N. B. (1942). Optimum settings for automatic controllers. *Transactions ASME*, *64*, 759–768.

Zuber, N., & Findlay, J. A. (1965). Average volumetric concentration in two-phase flow systems. *Journal of Heat Transfer*, *87*, 453–468.